Appl Phys B (2012) 106:267–270
DOI 10.1007/s00340-011-4695-9

Applied Physics B
Lasers and Optics

Amplification assisted optical parametric oscillator in the mid-infrared region

Y.H. Liu · X.J. Lv · Z.D. Xie · X.P. Hu · Y. Yuan · J. Lu · L.N. Zhao · G. Zhao · S.N. Zhu

Received: 2 May 2011 / Revised version: 28 June 2011 / Published online: 28 August 2011

Abstract We demonstrate a high efficiency mid-infrared laser source based on optical parametric oscillator (OPO) assisted by an intracavity optical parametric amplification (OPA). The OPA-assisted-OPO scheme was realized in one piece of commensurable dual-periodic superlattice in which the signal light generated from the OPO process serves as the pump light for the OPA process. A maximum output power of 508 mW at 3.92 μm was achieved under a pump power of 2.85 W at 1.064 μm. The pump-to-idler conversion efficiency is 17.8% and the slope efficiency is 23.8%, and the enhancements of them are 58.9% and 67.6%, respectively, comparing with the standard OPO scheme.

1 Introduction

Mid-infrared (IR) laser sources have many applications in the fields of environmental monitoring, medicine, spectroscopy, and infrared countermeasures. The quasiphase-matching technique is widely used in optical parameter oscillator (OPO) to obtain high-efficiency tunable mid-infrared lasers [1–4]. Most powerful mid-infrared OPOs are pumped by Nd-ion doped lasers with the pump wavelength of around 1 μm. According to the Manley–Rowe relations [5], the output power of the idler is greatly restricted by the quantum efficiency of converting for a conventional OPO process. For example, for the idler wavelength to be 4 μm, the maximum theoretic conversion efficiency from pump to idler is about 25%, and an experimental efficiency is reported to be about 10% by Dixit et al. [6]. To improve the conversion efficiency, some approaches have been employed. Phua et al. and Lancaster obtained efficiency enhancement by a $ZnGeP_2$ OPO pumped by a KTP-OPO, which in turn was pumped with 1 μm laser [7, 8]. Dearborn et al. reported an idler photon-conversion efficiency of 110% with the configuration of an OPO with intracavity difference-frequency mixing (DFG) [9]. However, they were accomplished with two different nonlinear crystals. Until Guo et al. proposed theoretically OPO, cascaded DFG simultaneously accomplished in a single optical superlattice obtained by aperiodically poling a ferroelectric crystal [10]. And then Porat et al. experimentally demonstrated improvement of the conversion efficiency by 16.6% with the OPO and DFG processes, in which quasiperiodic crystal employed was designed using the dual-grid method (DGM) [11, 12]. In this experiment, we demonstrate an OPA-assisted-OPO utilizing a stoichiometric $LiTaO_3$(SLT) optical superlattice with commensurable dual-periodic structure. The conversion efficiency reaches 17.8% and is improved by 58.9% comparing with standard OPO.

The mid-IR OPO was pumped by a 1.064 μm Nd:YAG laser. In order to improve the conversion efficiency from the near-IR to mid-IR, we used an intracavity OPA process to assist the OPO process. The first OPO process generated signal light at 1.46 μm and idler light at 3.9 μm, then the signal light served as the pump light of the OPA process to amplify the idler light at 3.9 μm. The OPA process operated in the OPO cavity, and enhanced the OPO process. Meanwhile, the enhanced OPO process would provide more pump light for the OPA process. Finally, the positive feedback of the two processes would greatly improve the conversion from the near-IR to mid-IR.

Y.H. Liu · X.J. Lv · Z.D. Xie · X.P. Hu · Y. Yuan · J. Lu · L.N. Zhao · G. Zhao · S.N. Zhu (✉)
National Laboratory of Solid State Microstructures and Department of Physics, Nanjing University, Nanjing, 210093, People's Republic of China
e-mail: zhusn@nju.edu.cn
Fax: +86-25-83595535

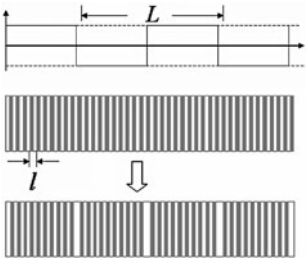

Fig. 1 Dual-periodic structure formed by modulation twice upon a periodic grating, where $l = 29.8$ μm, $L = 625.8$ μm and the ratio $L/l = 21$ is an integer

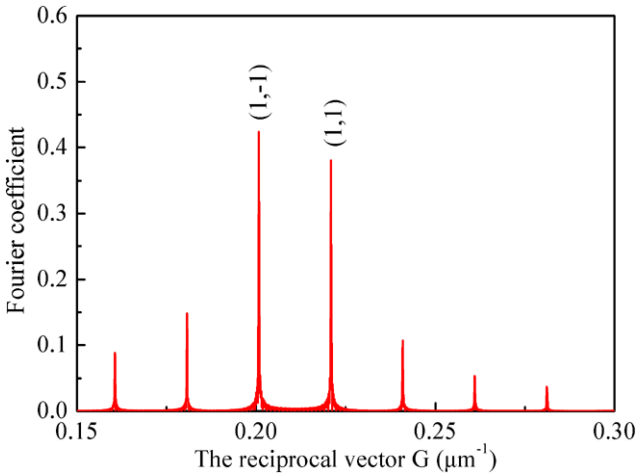

Fig. 2 Fourier spectrum of the dual-periodic structure. The two reciprocals marked with $(1, 1)$ and $(1, -1)$ are used to compensate for the phase mismatch for the OPO and OPA respectively

2 Structure design and characterization

We used a piece of commensurable dual-periodic superlattice to realize the OPO-OPA process. A dual-periodic structure can be described with a periodic domain-reversal sequence superimposed upon another smaller periodic structure [13, 14]. As shown in Fig. 1, the two periodic domain-reversal sequences are labeled as $F_1(x)$ and $F_2(x)$, which can be extended into two Fourier series:

$$F_1(x) = \sum_{m=-\infty}^{\infty} f_m e^{-iG_m x}, \qquad F_2(x) = \sum_{n=-\infty}^{\infty} f_n e^{-iG_n x} \tag{1}$$

The function of dual-periodic structure is defined as

$$F(x) = F_1(x) \times F_2(x) = \sum_{m,n=-\infty}^{\infty} f_{m,n} e^{-iG_{m,n} x} \tag{2}$$

where $f_{m,n} = f_m f_n$ are the Fourier coefficients. The reciprocals $G_{m,n}$ of the structure are given as $G_{m,n} = G_m + G_n = mG_l + nG_L$, where $G_l = 2\pi/l, G_L = 2\pi/L$ are the first-order reciprocals of the two periodic domain-reversal sequences. m, n are integers, which label the order of reciprocals. Usually, the periods of the two structures are not commensurable, and there will appear a small amount of tiny domains. The tiny domains will lead to domain merging during the electrical-poling process, and hence a reduction of the Fourier coefficients of the structure. If the two periods are commensurable, there will be no tiny domains that appear, thus the poling quality of the optical superlattice will be improved. In Fig. 1, the smaller period is $l = 29.8$ μm and the larger period is $L = 625.8$ μm, and we can see that L is 21 times that of l. The commensurable dual-periodic structure can provide a set of reciprocals $G_{m,n}$, and its Fourier spectrum can be obtained by Fourier transform of the dual-periodic sequence, as shown in Fig. 2. According to the temperature-dependent Sellmeier equation of SLT crystal [15], at the temperature of 180°C, we can calculate out that for the OPO process, i.e., 1.064 μm(λ_{pOPO}) → 1.457 μm(λ_{sOPO}) + 3.946 μm(λ_i), the wave vector mismatch is $\Delta k_{\mathrm{OPO}} = 0.2209$ μm^{-1}. While for the cascading OPA process, 1.457 μm(λ_{pOPA}) → 3.946 μm(λ_i) + 2.310 μm(λ_{sOPA}), the wave vector mismatch is $\Delta k_{\mathrm{OPA}} = 0.2008$ μm^{-1}. The two reciprocal vectors $G_{1,1}$ and $G_{1,-1}$ are used to compensate the phase mismatch for the OPO and OPA processes, respectively. The corresponding effective nonlinear coefficients for the two nonlinear processes are $d_{1,1} = 0.38d_{33}$ and $d_{1,-1} = 0.425d_{33}$, which ensure that both the processes can be effectively performed.

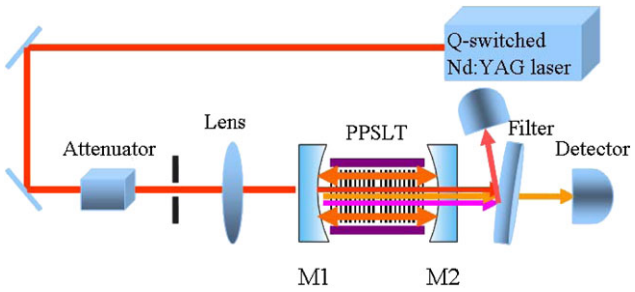

Fig. 3 Sketch map of the experiment setup. Attenuator, adjust the pump laser power onto the dual-periodic superlattice; Filter, used for spectrum-dividing

3 Experimental results and discussions

Figure 3 shows the schematic experimental setup of the OPA-assisted-OPO for mid-infrared generation. The pumping source is a Q-switched, linearly polarized Nd:YAG laser operating at 1064 nm with a pulse width of 40 ns and a repetition rate of 5 kHz. The OPA-assisted-OPO process is designed for signal single resonance. A 100-mm-long linear cavity consists of two mirrors M1 and M2 with a 100 mm radius of curvature. The two mirrors are both antireflection coated for 1.064 μm, 3.8–4.0 μm, and high-reflection coated ($R > 99.8\%$) for 1.4–1.5 μm. The commensurable dual-periodic optical superlattice (CDPOS) with dimensions

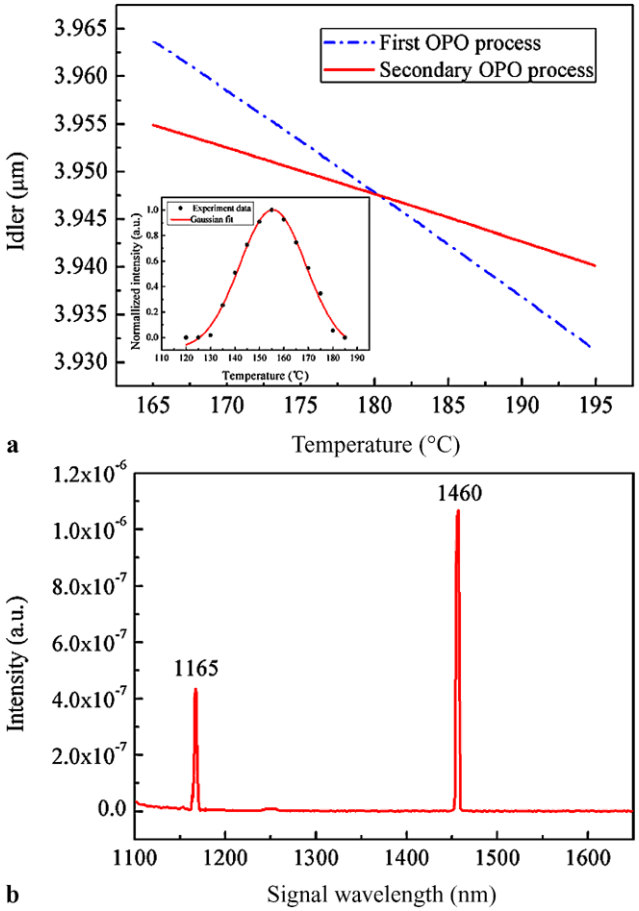

Fig. 4 (**a**) Idler wavelength tuning curves for the first OPO and second OPO processes. Insert is the measured temperature tuning curve for output λ_{s2} laser. (**b**) The output spectra at 155°C

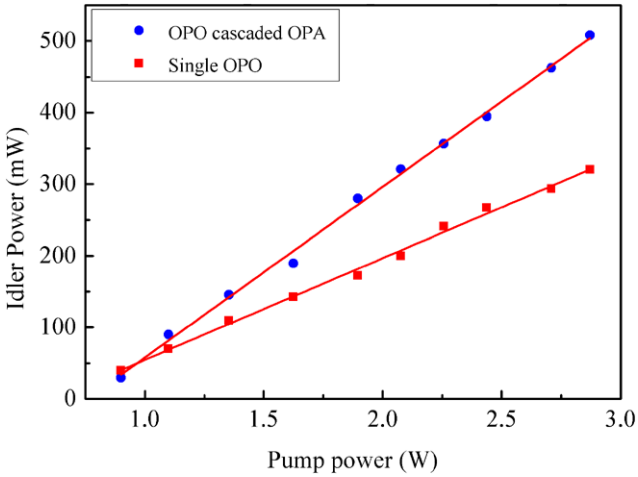

Fig. 5 Measured power dependence of the idler from the OPO-OPA process at 155°C and that from the single OPO at 175°C versus pump power

of 40 mm × 10 mm × 1 mm was fabricated in a single SLT crystal using electrical poling technique [16]. The two end-faces of the CDPOS were polished and antireflection coated at 1.064 μm, 1.4–1.5 μm, and 3.8–4.0 μm. Then the sample was imbedded in a temperature-controllable oven with an accuracy of ±0.1°C. A convex lens was used to focus the pump light onto the CDPOS and the beam waist inside the sample was estimated to be 200 μm. Meanwhile, the waist of the OPA-assisted-OPO cavity mode at 1.46 μm was calculated to be about 180 μm, which matched well with the beam waist inside the sample.

For the cascaded nonlinear process, parametric process pumped by 1.064 μm ($\lambda_p \rightarrow \lambda_{s1} + \lambda_{i1}$) occurs first, then the cascaded second parametric process ($\lambda_{s1} \rightarrow \lambda_{s2} + \lambda_{i2}$) will occur. The relations of λ_{i1} and λ_{i2} vary with the crystal temperature are shown in Fig. 4(a). When the two wavelengths get the same value, the signal and idler light of the first OPO serve as the pump and signal light of the second parametric process, respectively, and the OPO-OPA process is established. In the experiment, the OPO-OPA process occurs at 155°C, at other temperatures (e.g., 170°C), the second parametric process cannot be observed. The power dependence of λ_{s2} on the operating temperature is shown in the insert of Fig. 4(a). The measured results indicate that the maximum output power of λ_{s2} can be obtained at the temperature of 155°C, which demonstrates that OPO and OPA processes are simultaneously phase-matched. The spectra of the output beams recorded with an optical spectrum analyzer (ANDO AQ-6315A) are shown in Fig. 4(b). Due to the limitation of the measured span of the optical spectrum analyzer, we just acquired spectra of the signal at 1460 nm from the OPO process and the second harmonic wave (1165 nm) of 2.33 μm generated from OPA process. Actually, the coincident OPA-assisted-OPO process occurs as follows: 1.064 μm → 1.46 μm + 3.92 μm and 1.46 μm → 3.92 μm + 2.33 μm. The measured wavelengths are not exactly in agreement with the theoretical ones, which is mainly due to inaccuracies in the Sellmeier equation and not taking into account the thermal expansion of the crystal during calculations.

Then we set the temperature to be 155°C, the corresponding wavelength of the idler light was 3.92 μm. The power dependence of the idler on the pump at 1.064 μm was shown in Fig. 5. The threshold of the OPO-OPA process was measured to be 0.9 W and the maximum output power of the idler was about 508 mW. When the pump power reached 2.85 W, the mid-infrared conversion efficiency and the slope efficiency reached 17.8% and 23.8%, respectively. Then we tuned the CDPOS temperature to be 175°C far from the phase-matching point, owing to the coating properties of M1 and M2, and only the first OPO process occurred. The single OPO yielded a slope efficiency of 14.2% with a maximum idler output power of 320 mW at a pump power of 2.85 W, the corresponding conversion efficiency being 11.2%. Therefore, the conversion efficiency of OPO-OPA was supposedly improved over single OPO by 58.9%,

from 11.2% to 17.8%, and the slope efficiency improvement reached 67.6%. In the experiment, the highest power intensity was calculated to be 43 MW/cm^2, thanks to the high damaged threshold of SLT, which was reported to be 170 MW/cm^2 in our early work [17], which had a good coating quality, and we found no damage to the CDPOS in experiment. So, by increasing the pump power, we could acquire higher conversion efficiency, hence more output.

4 Summary

In conclusion, an OPA-assisted-OPO scheme was used to achieve 508 mW mid-IR laser light at around 3.92 μm with a specially designed commensurable dual-periodic optical superlattice simultaneously phase-matching the two nonlinear processes. High conversion efficiency up to 17.8% from pump to idler was obtained and the slope efficiency reached 23.8% in the single optical superlattice. This scheme can be easily scaled to higher power by further improving the pump power and optimizing the parameters of the cavity and superlattice structure.

Acknowledgements This work was supported by the State Key Program for Basic Research of China (2011CBA00205 and 2010CB630703) and the National Natural Science Foundation of China (NSFC) (10904066 and NSAF10776011).

References

1. R. Bhushan, H. Yoshida, K. Tsubakimoto, H. Fujita, M. Nakatsuka, N. Miyanaga, Y. Izawa, H. Ishizuki, T. Taira, Opt. Commun. **281**, 3902 (2008)
2. B. Wu, J. Kong, Y.H. Shen, Opt. Lett. **35**, 1118 (2010)
3. Y.F. Peng, W.M. Wang, X.B. Wei, D.M. Li, Opt. Lett. **34**, 2897 (2009)
4. T. Hatanaka, K. Nakamura, T. Taniuchi, Opt. Lett. **25**, 651 (2000)
5. J.M. Fraser, C. Ventalon, Appl. Opt. **45**, 4109 (2006)
6. N. Dixit, R. Mahendra, O.P. Naraniya, A.N. Kaul, A.K. Gupta, Opt. Laser Technol. **42**, 18 (2010)
7. P.B. Phua, K.S. Lai, R.F. Wu, T.C. Chong, Appl. Opt. **38**, 563 (1999)
8. D.G. Lancaster, Opt. Commun. **282**, 272 (2009)
9. M.E. Dearborn, K. Koch, G.T. Moore, Opt. Lett. **23**, 759 (1998)
10. H.C. Guo, Y.Q. Qin, Z.X. Shen, S.H. Tang, J. Phys., Condens. Matter **16**, 8465 (2004)
11. R. Lifshitz, A. Arie, A. Bahabad, Phys. Rev. Lett. **95**, 133901 (2005)
12. G. Porat, O. Gayer, A. Arie, Opt. Lett. **35**, 1401 (2010)
13. M.H. Chou, K.R. Parameswaran, M.M. Fejer, Opt. Lett. **24**, 1157 (1999)
14. Z.W. Liu, Y. Du, J. Liao, S.N. Zhu, Y.Y. Zhu, Y.Q. Qin, H.T. Wang, J.L. He, C. Zhang, N.B. Ming, J. Opt. Soc. Am. B **19**, 1676 (2002)
15. A. Bruner, D. Eger, M.B. Oron, P. Blau, M. Katz, S. Ruschin, Opt. Lett. **28**, 194 (2003)
16. S.N. Zhu, Y.Y. Zhu, Z.Y. Zhang, H. Shu, H.F. Wang, J.F. Hong, C.G. Ge, N.B. Ming, J. Appl. Phys. **77**, 5481 (1995)
17. X.P. Hu, X. Wang, J.L. He, Y.X. Fan, S.N. Zhu, H.T. Wang, Y.Y. Zhu, N.B. Ming, Appl. Phys. Lett. **85**, 188 (2004)